

Measurements of Compton Scattered Transition Radiation at High Lorentz Factors

Gary L. Case,^{1,*} P. Parker Altice,^{1,†} Michael L. Cherry,¹ Joachim Isbert,¹ John W. Mitchell,² and Donald Patterson¹

¹*Dept. of Physics and Astronomy, Louisiana State University, Baton Rouge, LA 70803*

²*NASA Goddard Space Flight Center, Greenbelt, MD 20771*

(Dated: February 8, 2020)

X-ray transition radiation can be used to measure the Lorentz factor of relativistic particles. Standard transition radiation detectors (TRDs) typically incorporate thin plastic foil radiators and gas-filled x-ray detectors, and are sensitive up to $\gamma \sim 10^4$. To reach higher Lorentz factors (up to $\gamma \sim 10^5$), thicker, denser radiators can be used, which consequently produce x-rays of harder energies ($\gtrsim 100$ keV). At these energies, scintillator detectors are more efficient in detecting the hard x-rays, and Compton scattering of the x-rays out of the path of the particle becomes an important effect. The Compton scattering can be utilized to separate the transition radiation from the ionization background spatially. The use of conducting metal foils is predicted to yield enhanced signals compared to standard nonconducting plastic foils of the same dimensions. We have designed and built a Compton Scatter TRD optimized for high Lorentz factors and exposed it to high energy electrons at the CERN SPS. We present the results of the accelerator tests and comparisons to simulations, demonstrating 1) the effectiveness of the Compton Scatter TRD approach; 2) the performance of conducting aluminum foils; and 3) the ability of a TRD to measure energies approximately an order of magnitude higher than previously used in very high energy cosmic ray studies.

INTRODUCTION

Transition radiation (TR) is produced when a charged particle crosses the interface between two materials with different dielectric constants, resulting in the rapid rearrangement of the particle's electric field as it passes from one material to the next. Detailed calculations of the TR phenomenon are given in the literature (e.g. [1, 2, 3]); only the relevant properties are summarized here. For highly relativistic particles ($\gamma = E/mc^2 \gg 1$) the radiation is emitted at x-ray frequencies. The spectrum produced depends on the plasma frequencies and thicknesses of the two materials as well as the energy of the particle. Typically, the materials used are a low atomic number solid such as plastic, with plasma frequency ω_1 , and a gas or vacuum with plasma frequency ω_2 . Radiation is emitted up to a frequency $\gamma\omega_1$, beyond which the spectrum is suppressed. The total intensity produced from a single interface is proportional to $Z^2\gamma$, where Z is the charge of the particle.

The intensity of the TR from a single interface is weak. Therefore, in practical applications, a radiator is constructed with a large number N of thin foils of thickness l_1 separated by a distance l_2 , with TR produced at each of the $2N$ interfaces. Interference effects from the superposition of the amplitudes produced at each interface give rise to pronounced minima and maxima in the spectrum, with the last (highest frequency) maximum near

$$\omega_{\max} = \frac{l_1\omega_1^2}{2\pi c}(1 + \rho), \quad (1)$$

where ρ is 1 for a metal and 0 for a nonconductor. A nonzero conductivity introduces an imaginary part to the wave vector, which leads to an effective increase in the plasma frequency, $\omega_1\sqrt{1 + \rho}$ [4]. As the particle energy

increases, the total radiated intensity increases up to a Lorentz factor

$$\gamma_s \approx \frac{0.6\omega_1}{c}\sqrt{l_1l_2(1 + \rho)}, \quad (2)$$

above which saturation sets in due to the interference. The saturation energy and characteristic frequency can be tuned by varying the radiator foil material, thickness, and separation.

An x-ray detector appropriate for absorbing the TR x-rays must be placed after the radiator. The radiation is emitted at an angle $\theta \approx 1/\gamma$ with respect to the incident particle direction, so the x-rays are coincident with the ionization energy deposited in the detector by the particle itself. Therefore, in conventional applications, the detector must be made thin in order to minimize the ionization signal, yet with sufficient stopping power to absorb the x-rays. For ω_{\max} less than ≈ 40 keV, gas detectors (e.g. Xenon-filled wire chambers) are typically employed. In order to improve statistics and for redundancy, a complete transition radiation detector (TRD) consists of multiple layers of radiators and x-ray detectors. Such TRDs have been used successfully both at accelerators and in space, where the energies of cosmic ray nuclei with $\gamma \geq 3 \times 10^3$ have been measured by the Space Shuttle CRN experiment [5, 6]. An extensive review of TR applications is given by [7], and a brief listing of cosmic ray experiments using TRDs is given in [8].

It is important to develop the capability to measure the energies of particles with Lorentz factors $\gamma \sim 10^5$. For example, NASA's proposed Advanced Cosmic Ray Composition Experiment for Space Science (ACCESS) mission [9, 10, 11] requires a TRD capable of measuring the energies of cosmic rays up to 100 TeV/nucleon for $Z > 3$. The range of existing TRDs must be extended upward by an order of magnitude or more, requiring designs modi-

fied for use at these higher energies. In order to increase the maximum particle energy γ_s , one must increase the plasma frequency (or equivalently, density), thickness, and/or spacing of the foils (Eq. 2). In a space instrument, the overall thickness will be constrained, putting a limit on Nl_2 (assuming $l_2 \gg l_1$). Increasing ω_1 (i.e. using metal foils instead of plastic) and/or l_1 results in a hardening of the x-ray spectrum produced (Eq. 1). Metal foils have been used in early accelerator tests [12], and in particular lithium foils have been used in accelerator applications in order to minimize the absorption at low x-ray frequencies [13, 14]. In the case of very high energies, though, with $\gamma_s \approx 10^5$ and a typical spacing $l_2 = 0.1 - 1$ cm, $\omega_{\max} \approx 0.4\gamma_s^2 c/l_2$ can be in excess of several hundred keV. Gas detectors are then no longer efficient in detecting these hard x-rays. Although [15] describes the use of gas detectors near $\gamma_s \approx 10^5$ by optimizing the radiator design, scintillators such as NaI or CsI provide an efficient alternative at these Lorentz factors and corresponding high x-ray energies. The higher density of the scintillators leads to an increase in the ionization energy deposited by the particle as it traverses the detector. However, as the TR spectrum hardens, Compton scattering in the radiators becomes important, becoming the dominant photon interaction above ≈ 40 keV. A significant portion of the x-rays produced are scattered out of the path of the incident particle. Thus, a detector that is segmented or positioned outside of the beam can efficiently detect the TR signal spatially separated from the ionization.

We describe here the test of a scintillator-based Compton Scatter TRD for high Lorentz factor particles, including the use of metal foils, based on the results of accelerator measurements with high energy electrons at the CERN SPS. Comparisons of the measured results with detailed simulations will also be presented.

INSTRUMENT DESCRIPTION AND EXPERIMENTAL SETUP

A scintillator-based Compton Scatter TRD was designed to investigate the predicted increase in saturation energy obtained by using thick, dense radiator materials. Materials investigated included Mylar ($\rho = 1.4$ g/cm³), Teflon ($\rho = 2.0$ g/cm³) and aluminum ($\rho = 2.7$ g/cm³). The use of metal foils is of particular interest as the nonzero conductivity should produce a characteristic enhancement in the signal [4].

For the plastics, radiator stacks of $N = 50$ foils were constructed by attaching 19.1 cm \times 18.4 cm plastic foils to 3.4 mm thick balsa wood frames and stacking the frames together. For the aluminum, each radiator stack consisted of seven 1" thick honeycomb panels bundled together and aligned with the cells perpendicular to the particle beam. The honeycomb was a composite mate-

TABLE I: Parameters of radiator configurations tested

Radiator	ω_1 (eV)	l_1 (μ m)	l_2 (mm)	N	ω_{\max} (keV)	γ_s
Thin Mylar	24.4	125	3.4	50	61	4.9×10^4
Thick Mylar	24.4	250	3.4	50	122	6.9×10^4
Thin Teflon	28.5	125	3.5	50	83	5.8×10^4
Thick Teflon	28.5	200	3.4	50	133	7.2×10^4
Aluminum	32.7	135	3.8	48	230	9.9×10^4

rial chosen both for its dimensions and its adaptability as a combined detector-plus-structure for a space instrument. Particles passing through the structure (Fig. 1) passed through either 1) a section of foils perpendicular to the beam in which two 0.003" sheets glued together form a foil with an effective $l_1 = 0.006"$, $l_2 = 5.2$ mm, and $N = 35$ foils along the particle trajectory or 2) a section of foils at a 41° angle with respect to the particle beam, resulting in an effective foil thickness $l_1 = 0.003"/\sin 41^\circ = 0.0046"$, l_2 ranging from 0 to 5.2 mm, and $N = 70$. The yield from a composite material (e.g. a foam) with average values $\langle l_1 \rangle$, $\langle l_2 \rangle$, and $\langle N \rangle$ has been shown to be essentially the same as from a regular foil radiator with the same l_1 , l_2 , and N [16]. We therefore calculate the aluminum honeycomb effective parameters as averages of configuration 1 weighted by 46% (to account for the fraction of the area perpendicular to the beam covered by configuration 1) and configuration 2 weighted by 54%. The resulting average honeycomb radiator parameters are given in Table I, along with the parameters of the plastic radiator configurations tested. The total length of each radiator stack was 19 cm.

Each radiator stack was viewed by three x-ray detec-

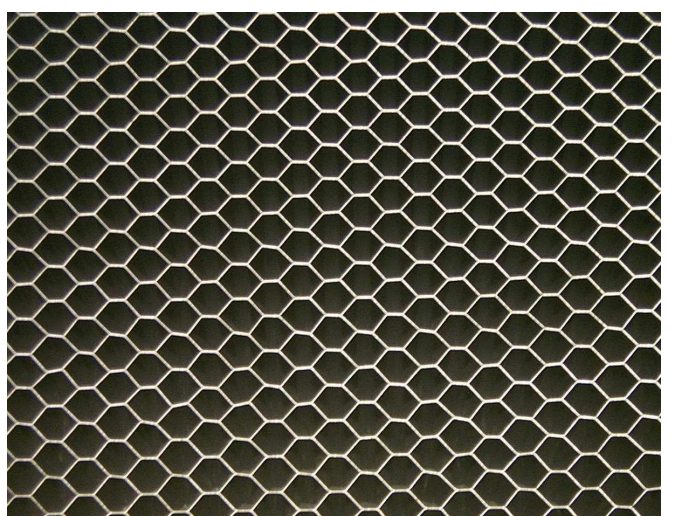


FIG. 1: Photograph of an aluminum honeycomb panel. The particle trajectory is from the top to bottom.

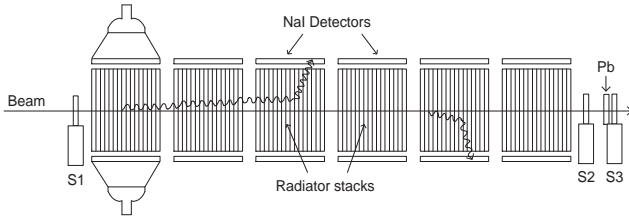


FIG. 2: Schematic of the experimental setup, as seen from above. Lightguide and PMT assemblies are shown for the first module only. An additional NaI detector (not shown) was positioned above each radiator stack. The location of the beam definition scintillators S1 and S2 and shower counter S3 are also shown. TR x-rays are produced in the forward direction and can Compton scatter out of the beam and into the NaI scintillators.

tors, each consisting of a $19\text{ cm} \times 19\text{ cm} \times 5\text{ mm}$ thick NaI(Tl) crystal hermetically sealed between a 6.4 mm thick glass optical window on one flat face and a 0.75 mm thick aluminum entrance window on the other face. An ultraviolet transmitting Lucite lightguide was coupled to the glass window using optical grease, reducing the aperture to a 13 cm diameter circle. An Electron Tubes 9390KB 130 mm photomultiplier tube with a standard bialkali photocathode was mated to the lightguide with optical grease. The lightguide was wrapped in aluminum foil and the whole assembly wrapped with black tape to make it light tight.

Six identical TRD modules were constructed, with each module containing a radiator stack and the three NaI(Tl) detector assemblies: one on each side of the radiator stack and one above the stack outside of and parallel to the beam (Fig. 2). The modules were positioned along the beam and aligned such that the particle beam travelled down the center of the modules. Only x-rays scattered at large angles away from the beam were then detected.

For the first accelerator run, the 18 PMT signals were fed into CAMAC-based, 12-bit charge ADCs and read out with the CERN CMS H2A DAQ computer. For the second accelerator run, the signals from the PMTs were fed into custom-built 8-channel front end modules, which contained a charge integrator, peak detect and hold circuit, and gain-adjustable amplifier. Analog-to-digital conversion was performed with a 64 channel, 12-bit National Instruments PCI-6071E DAQ board running in a PC under LabVIEW 6i. Consistent results were obtained with the two electronic systems.

The instrument was exposed to high energy electrons at the CERN SPS H2A test beam site in August/September 1999 and again in August/September 2001. Beam energies ranged from 7 to 150 GeV, covering the range of Lorentz factors $\gamma = 1.4 \times 10^4 - 2.9 \times 10^5$. A set of scintillators in the beam upstream of the TRD provided event triggering. The trigger rate was kept to about 1 kHz to avoid deadtime in the DAQ system. Beam defi-

nition scintillators were set up in front of and behind the TRD (S1 and S2 in Fig. 2). The data from these detectors were used during analysis to flag events for which the electrons showered within the radiator stacks. A Pb shower counter (S3) was placed downstream of S2 to flag pions present as a contaminant in the higher energy beams. Energy calibration runs were performed both immediately before and after the beam runs using radioac-

tive sources.

In order to account for bremsstrahlung and other background produced by the electrons in passing through the radiators and upstream material, a background run was performed for each radiator configuration in which the radiators were replaced by solid blocks with the same material and thickness (in g/cm^2) as the radiators.

RESULTS

Data were taken at various electron energies for each radiator configuration. Not every configuration was run at all of the available electron energies due to time constraints in sharing the beam with other experiments. For each material, a background run and a foil run were made for each electron energy used. The background data were scaled to and then subtracted from the foil data in order to obtain the signal due to TR. Figure 3 shows the spectra obtained from a single downstream detector (in the fifth module) for aluminum foil and background runs at 150 GeV. Two things are immediately evident: first, Compton scattered transition radiation is being detected away from the path of the incident electron; and second, the detected TR x-ray spectrum peaks about 120 keV, with some x-rays detected at energies > 300 keV.

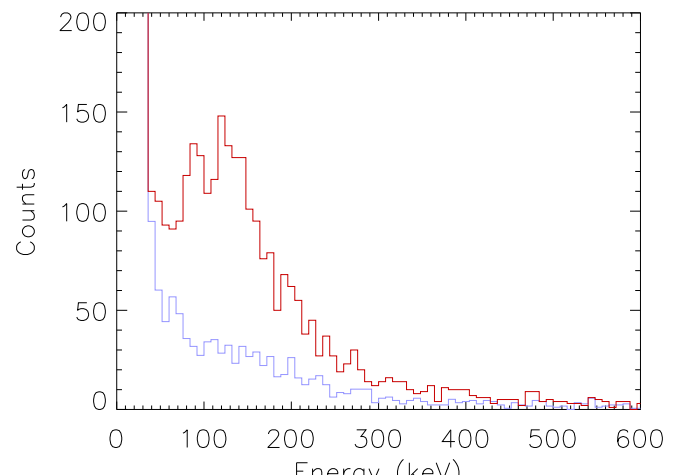


FIG. 3: Spectra measured in a single downstream detector using 150 GeV electrons with aluminum honeycomb radiators (upper curve) and solid aluminum background plates (lower curve).

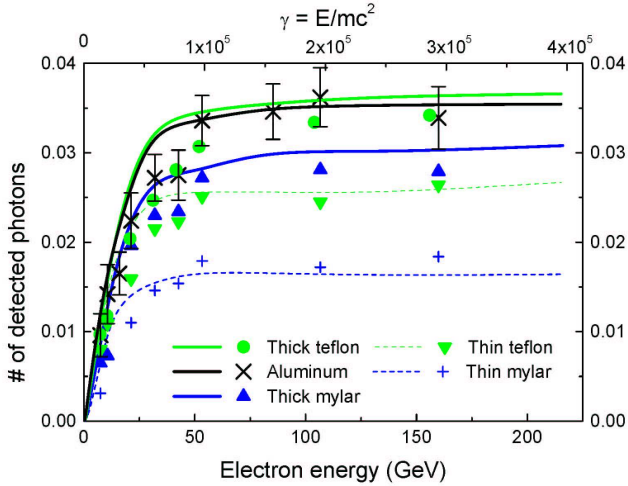


FIG. 4: Average number of photons detected in the energy range 35 – 500 keV per detector per event in the first module as a function of electron energy for various radiator configurations. The symbols represent experimental data and solid lines represent results of calculations. The error bars represent statistical errors.

The number of x-rays measured in each detector depends on the position of the module. TR x-rays produced in the beginning of the first module can pass through that module without interacting (73% probability in an aluminum honeycomb radiator at 100 keV). But as they encounter the radiator material in successive modules, they can Compton scatter and be absorbed in a downstream detector. For the aluminum honeycomb, there is an 80% probability that a 100 keV x-ray created at the front of the first module will Compton scatter in the radiators before leaving the last module. This feedthrough effect then enhances the number of photons detected in modules downstream. For 150 GeV electrons and aluminum honeycomb radiators, over the x-ray energy range 35 – 500 keV, 4.2 times more photons were detected on average in module 6 than in the first module.

In order to compare the detected yields of the different radiator configurations, the total number of photons detected per NaI detector was summed over the energy range 35 – 500 keV. Figure 4 shows the detected yields as a function of electron energy. The points show the measured data; the curves show the results calculated as described in [4], including the effects of photoelectron statistics, photoelectric absorption, Compton scattering, fluorescence and escape in both the detectors and radiators. The observed saturation Lorentz factors for the thick Teflon and aluminum honeycomb are $\approx 10^5$, as expected from the calculated values in Table I. The calculations predicted well the differences in detected yield between different radiator materials and between different thicknesses of the same material.

CONCLUSION

A new Compton Scatter Transition Radiation Detector capable of measuring the x-rays produced by particles with Lorentz factors near $\gamma = 10^5$ has been built and successfully tested. Compton scattered TR x-rays were detected outside of the particle beam using relatively thick NaI scintillator detectors, effectively isolating the TR signal from the ionization signal. For the thick Teflon and aluminum honeycomb radiators, the detected x-ray spectrum peaks near 100 keV with some x-rays > 300 keV detected, and saturation Lorentz factors near 10^5 were achieved. The detected yields for various radiator configurations agree with detailed simulations, including the enhancement expected from metal foils.

This work was supported by NASA grant NAG5-5177 and NASA/Louisiana Board of Regents grant NASA/LEQSF-IMP-02. The authors wish to thank A. Aranas, S. Apewokin, T. Brown and O. Shertukde for their many hours of work during the construction and testing of the radiators and detectors; the staff at CERN for their superb cooperation and assistance, particularly D. Lazic and G. Bencze; and J. Anderson, J. Marsh and C. Welch for assisting with the data analysis.

* Email address: case@phunds.phys.lsu.edu

† Current address: Micron Technology, Boise, ID 83707

- [1] M. L. Ter-Mikaelian, *High Energy Electromagnetic Processes in Condensed Media* (Wiley, New York, 1972).
- [2] M. L. Cherry, Phys. Rev. D **17**, 2245 (1978).
- [3] X. Artu, G. Yodh, and G. Mennessier, Phys. Rev. D **12**, 1289 (1975).
- [4] M. L. Cherry and G. L. Case, Astroparticle Physics pp. to be published, astro-ph/0206063 (2002).
- [5] J. M. Grunsfeld, J. L'Heureux, P. Meyer, D. Müller, and S. P. Swordy, Astrophys. J. Lett. **327**, L31 (1988).
- [6] S. P. Swordy et al., Phys. Rev. D **42**, 3197 (1990).
- [7] C. Favuzzi, N. Giglietto, N. M. Mazziotta, and P. Spinelli, La Rivista del Nuovo Cimento **24**, 1 (2001).
- [8] M. L. Cherry and J. P. Wefel, in *Proc. TRDs for the 3rd Millennium*, edited by N. Giglietto and P. Spinelli (2002), vol. XXV of *Frascati Physics Series*, p. 151.
- [9] J. P. Wefel and T. L. Wilson, in *Proc. 26th Intl. Cosmic Ray Conf.* (Salt Lake City, 1999), vol. 5, p. 84.
- [10] M. Israel et al., NASA GSFC report NP-2000-05-056-GSFC (2000).
- [11] T. L. Wilson and J. P. Wefel, NASA report TP-1999-209202 (1999).
- [12] L. C. L. Yuan, C. L. Wang, and S. Prunster, Phys. Rev. Lett. **23**, 496 (1969).
- [13] J. Fischer et al., Phys. Lett. B **49**, 393 (1974).
- [14] J. Cobb et al., Nucl. Instrum. Meth. **140**, 413 (1977).
- [15] S. P. Wakely, Astroparticle Physics **18**, 67 (2002).
- [16] T. A. Prince, D. Müller, G. Hartmann, and M. L. Cherry, Nucl. Instrum. Meth. **123**, 231 (1975).